

# Superconductivity in striped and multi-Fermi-surface Hubbard models: From the cuprates to the pnictides

Thomas A. Maier

Received: date / Accepted: date

**Abstract** Single- and multi-band Hubbard models have been found to describe many of the complex phenomena that are observed in the cuprate and iron-based high-temperature superconductors. Simulations of these models therefore provide an ideal framework to study and understand the superconducting properties of these systems and the mechanisms responsible for them. Here we review recent dynamic cluster quantum Monte Carlo simulations of these models, which provide an unbiased view of the leading correlations in the system. In particular, we discuss what these simulations tell us about superconductivity in the homogeneous 2D single-orbital Hubbard model, and how charge stripes affect this behavior. We then describe recent simulations of a bilayer Hubbard model, which provides a simple model to study the type and nature of pairing in systems with multiple Fermi surfaces such as the iron-based superconductors.

**Keywords** Superconductivity · Cuprates · Pnictides

Phenomenologically, the cuprate and iron-based high-temperature superconductors share in common that superconductivity occurs by doping into an antiferromagnetic Mott or spin density wave state. The magnetism in these compounds originates from partially filled Cu or Fe d-orbitals which energetically lay at the Fermi energy. A reasonable starting point for a theoretical description of these compounds is therefore given by a Hubbard model which describes moment formation due to a strong local Coulomb repulsion between the electrons on the d-orbitals. In the case of the cuprates,

a single electronic band mainly of Cu  $d_{x^2-y^2}$ -character crosses the Fermi surface and a single-band Hubbard model has therefore been argued to provide a simple framework to describe the low-energy physics of this class of materials [1,18]. In the iron-based materials, one has multiple Fermi surfaces formed by Bloch states originating from several of the iron d-orbitals. Therefore, one needs to start with a multi-orbital Hubbard model to describe the more complex electronic structure of these systems [5,10]. A two-band model has also been used to study phase separation in cuprate superconductors [9].

Here, we review recent dynamic cluster quantum Monte Carlo calculations of these models [14,15,12,16]. In particular, we will focus on what these simulations tell us about the nature of pairing and the effect of charge stripes in the single-band 2D Hubbard model, as well as the leading pairing correlations in a bilayer Hubbard model with multiple Fermi surfaces.

The Hamiltonian for the 2D Hubbard model we will study can be written as

$$\mathcal{H} = -t \sum_{\langle ij \rangle, \sigma} (c_{i\sigma}^\dagger c_{j\sigma} + h.c.) + U \sum_i n_{i\uparrow} n_{i\downarrow}. \quad (1)$$

Here  $t$  is a nearest neighbor hopping parameter,  $U$  is an on-site Coulomb repulsion and  $\langle ij \rangle$  implies summation over nearest neighbor pairs only. In the following we will measure energies in units of  $t$ . The single band with dispersion  $\varepsilon_k = -2t(\cos k_x + \cos k_y)$  describes the electronic states near the Fermi energy in the cuprate materials.

As discussed in the introduction, a realistic description of the pnictides requires a multi-orbital Hubbard model describing the 5 iron d-orbitals near the Fermi energy and their intra- and inter-orbital Coulomb, Hund's rule and pair hopping interactions. Such a model is too

---

Thomas A. Maier  
 Computer Science and Mathematics Division and Center for  
 Nanophase Materials Sciences  
 Oak Ridge National Laboratory Tel.: +865-539-6868  
 E-mail: maierta@ornl.gov

complex to simulate with quantum Monte Carlo approaches, and so we will instead study a simpler two-orbital model with only intra-orbital Coulomb interactions. This model will be realized by a bilayer Hubbard model. Its Hamiltonian is given by

$$H = -t \sum_{\langle ij \rangle m \sigma} (c_{im\sigma}^\dagger c_{jm\sigma} + \text{h.c.}) - t_\perp \sum_{i\sigma} (c_{i1\sigma}^\dagger c_{i2\sigma} + \text{h.c.}) + U \sum_{im} n_{im\uparrow} n_{im\downarrow}. \quad (2)$$

Here the layers are indexed by  $m$ , each layer is described by the Hamiltonian in Eq. 1 and  $t_\perp$  is an additional hopping parameter between neighboring sites in the bi-layer model. This model provides a simplified two-orbital system in which one can study the type of pairing that can occur in systems with multiple Fermi surfaces such as the iron-pnictides.

In order to analyze these models, we will use a dynamic cluster quantum Monte Carlo approximation (DCA/QMC) [6, 8, 13]. The DCA maps the bulk lattice problem onto an effective periodic cluster embedded in a dynamic mean-field that is designed to represent the rest of the system. The effective cluster problem is then solved using a quantum Monte Carlo algorithm. The results discussed in this paper were obtained with a Hirsch-Fye method [8]. DCA/QMC calculations of the 2D Hubbard model have found many phenomena that are also observed in the cuprates, including an antiferromagnetic Mott state, d-wave superconductivity as well as pseudogap behavior [13]. It therefore provides an interesting framework to study many of the open questions in the field.

Formally, the quantity of interest to study the nature of pairing in these models is given by the two-particle irreducible vertex in the particle-particle channel,  $\Gamma_{\text{irr}}^{pp}(k, k')$  [14]. Here  $k = (\mathbf{k}, i\omega_n)$  with  $\omega_n$  a fermion Matsubara frequency and we are interested in the singlet pairing channel. This quantity describes the scattering of two electrons with momenta  $\mathbf{k}$  and  $-\mathbf{k}$  and anti-parallel spins to a state with momenta  $\mathbf{k}'$  and  $-\mathbf{k}'$  and therefore describes the pairing interaction. Together with the single-particle Green's function  $G(k)$ , it enters the Bethe-Salpeter equation

$$-\frac{T}{N} \sum_k \Gamma_{\text{irr}}^{pp}(k, k') G(k') G(-k') \Phi_\alpha(k') = \lambda_\alpha \Phi_\alpha(k) \quad (3)$$

which provides information on the strength ( $\lambda_\alpha$ ) and momentum and frequency structure ( $\Phi_\alpha(k)$ ) of the leading pairing correlations in the system [14]. At  $T_c$ ,  $\lambda_\alpha = 1$  and  $\Phi_\alpha(k)$  becomes identical to the superconducting gap. In the 2D Hubbard model, at low temperature, one finds that the eigenvector corresponding to the leading eigenvalue has a d-wave  $\cos k_x - \cos k_y$  momentum dependence.

Previous DCA/QMC simulations of the 2D Hubbard model [14, 15] have found that the momentum and frequency dependence of the pairing interaction  $\Gamma_{\text{irr}}^{pp}(k, k')$  is similar to that of the spin susceptibility  $\chi(k - k')$ , providing evidence that that pairing interaction in this model is carried by spin fluctuations.

In a spin fluctuation picture, one can naturally understand the drop of  $T_c$  with doping on the overdoped side of the cuprate phase diagram, since the spin-fluctuations are weakened by doping away from the antiferromagnetic parent state. On the other hand, the drop of  $T_c$  with underdoping is difficult to understand in a picture where pairing is mediated by spin fluctuations, since one would expect them to get stronger when the system is doped towards the Mott state. To investigate this issue we show in Fig. 1a the temperature versus doping superconducting phase diagram of the 2D Hubbard model, calculated with DCA/QMC on an 8-site cluster with  $U=8$ . One sees that these calculations correctly predict the experimentally observed dome-like structure of the superconducting phase diagram, with  $T_c$  dropping with both over- and underdoping.

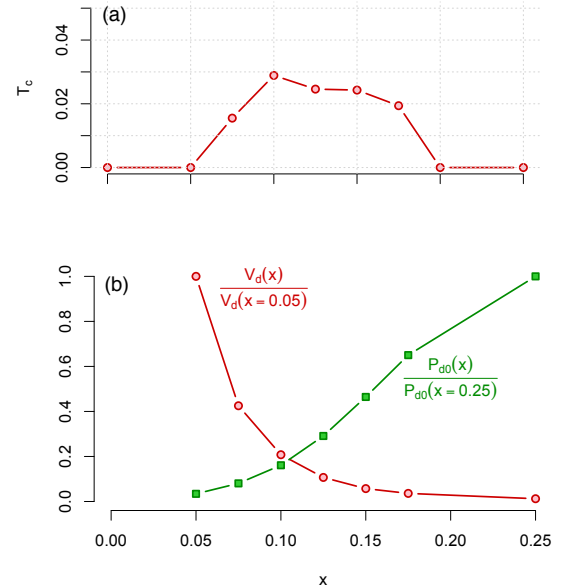


**Fig. 1** (a) Superconducting transition temperature  $T_c$  versus doping  $x$  for the 2D Hubbard model with  $U = 8$  calculated with DCA/QMC on an 8-site cluster. (b) Normalized interaction strength  $V_d$  and "intrinsic" pair-field susceptibility  $P_{d,0}$  versus doping  $x$  calculated at a temperature  $T = 0.125$ .

In order to analyze how this behavior arises from the Bethe-Salpeter equation (3), we have calculated the "intrinsic" pair-field susceptibility projected onto the

leading eigenvector,  $P_{d,0} = T/N \sum_k \Phi_d(k)^2 G(k)G(-k)$  and the strength of the pairing interaction  $V_d$  from  $V_d P_{d,0} = \lambda_d$ . The doping dependence of these quantities calculated at a low temperature above  $T_c$  are shown in Fig. 1b. As one would expect from a spin-fluctuation based pairing interaction,  $V_d$  rises monotonically with decreasing doping towards the Mott insulator. In contrast,  $P_{d,0}$  decreases with decreasing doping and goes to zero as one approaches the Mott state. The drop of  $T_c$  on the underdoped side therefore is caused by the strong Mott quasiparticle renormalization when the doping is close to zero.

Despite the strong pairing interaction  $V_d$  in the underdoped system,  $T_c$  is small because of the Mott quasiparticle degradation. It has been suggested that in this case,  $T_c$  may be enhanced in a striped state, in which the system is separated into hole-rich regions with good hole mobility, and hole-poor regions with strong anti-ferromagnetic correlations. To explore this prediction, we have performed DCA/QMC calculations of a striped  $8 \times 4$ -site cluster [12]. The charge stripes were imposed by hand, by adding a site-dependent external potential  $V_i$  that couples to the charge density on site  $i$ .  $V_i$  is chosen to have a maximum amplitude  $V_0$  and to vary smoothly along the long 8-site x-direction of the cluster while being constant along the 4-site y-direction. The variation of  $V_i$  along the x-direction is shown at the bottom of Fig. 2a. Here we are interested in a striped inhomogeneity with period 8. The calculated site-filling is displayed at the top of Fig. 2a and found to follow closely the variation of the external potential.

In order to keep the problem computationally tractable, we have averaged over different stripe origins along the x-direction, before computing the mean-field medium [12]. This corresponds to a situation where the stripe order is short-ranged, over the length-scale of the cluster, but is translationally invariant on longer macroscopic length scales.

The temperature dependence of the leading (d-wave) eigenvalue of the Bethe-Salpeter equation (3) computed for different amplitudes  $V_0$  of the potential is shown in Fig. 2b. As one can see, the pairing correlations are indeed enhanced by the charge stripe and  $T_c$ , i.e. the temperature where  $\lambda_d(T)$  crosses 1, is increased. One also sees that there is an optimum inhomogeneity at around  $V_0 = 0.4$  for which  $T_c$  is maximized. For larger  $V_0$ ,  $T_c$  is found to drop again.

Finally, we discuss recent DCA/QMC results for the bilayer Hubbard model [16]. This model provides a simple system with multiple Fermi surfaces, in which one can study the type of pairing that can occur in systems such as the iron-pnictides. Due to the inter-layer

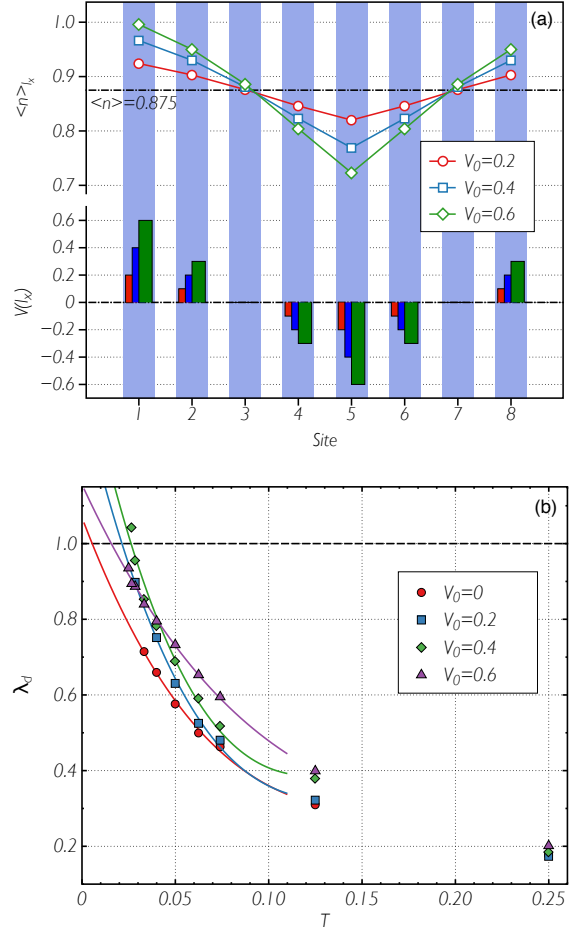


**Fig. 2** DCA/QMC simulation of an inhomogeneous  $8 \times 4$  cluster with a charge stripe. (a) External potential  $V(l_x)$  and resulting charge density  $\langle n \rangle_{l_x}$  along the long (8-site) direction of the cluster for different magnitudes  $V_0$ . (b) Leading eigenvalue of the particle-particle Bethe-Salpeter equation (3) versus temperature for different  $V_0$ .

hopping  $t_\perp$ , one has a bonding and an anti-bonding band split by  $2t_\perp$  for  $U = 0$ . The bonding and anti-bonding Fermi surfaces of the non-interacting system are shown in Fig. 3 (a) and (b) for a filling  $\langle n \rangle = 0.95$  and two values of  $t_\perp/t$ . As  $t_\perp/t$  increases the Fermi surfaces shrink and for  $\langle n \rangle = 1$  the non-interacting system becomes a band-insulator for  $t_\perp > 4$ . Weak coupling calculations for the doped system [3,11] have found a  $d_{x^2-y^2}$ -like gap for  $t_\perp/t = 0.5$  and a fairly isotropic "s $^\pm$ " gap that changes sign between the bonding and anti-bonding Fermi surfaces for  $t_\perp/t = 2.0$ , as schematically illustrated in Fig. 3 (a) and (b).

Here we describe the results of DCA/QMC calculations which provide an unbiased treatment of this model and allow us to reach lower temperatures than previous finite size quantum Monte Carlo calculations [3,17,7,4,

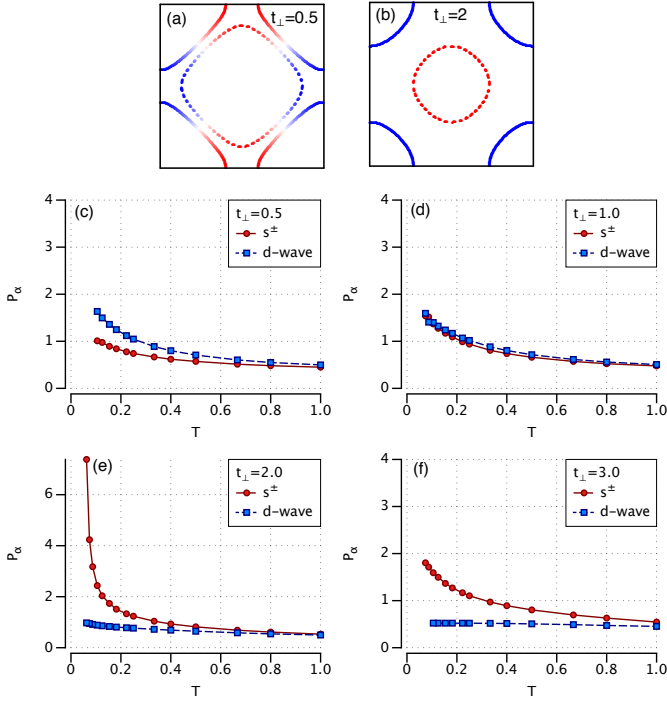


**Fig. 3** DCA/QMC simulation of a bilayer Hubbard model with inter-layer hopping  $t_{\perp}$ . The bonding (solid lines) and anti-bonding (dashed lines) Fermi surfaces of the non-interacting system for (a)  $t_{\perp} = 0.5$  and (b)  $t_{\perp} = 2$  for a filling  $\langle n \rangle = 0.95$ . A  $d_{x^2-y^2}$  gap structure is illustrated in for the  $t_{\perp}/t = 0.5$  Fermi surface and an  $s^{\pm}$  gap structure is shown for  $t_{\perp}/t = 2.0$ . (c) The  $d$ -wave and  $s^{\pm}$  pair-field susceptibilities  $P_{\alpha}$  versus temperature for different values of the inter-layer hopping  $t_{\perp}$ . As  $t_{\perp}$  increases, the leading instability changes from  $d$ -wave to  $s^{\pm}$  and at larger values of  $t_{\perp}$  the superconducting pair-field susceptibility is suppressed.

2]. The superconducting response is studied by calculating the pairfield susceptibility

$$P_{\alpha}(T) = \int_0^{\infty} d\tau \langle \Delta_{\alpha}(\tau) \Delta_{\alpha}^{\dagger}(0) \rangle. \quad (4)$$

Here  $\Delta^{\dagger} = 1/\sqrt{N} \sum_k g(k) c_{k\uparrow}^{\dagger} c_{-k\downarrow}^{\dagger}$  and  $g(k) = \cos k_x - \cos k_y$  for the  $d_{x^2-y^2}$ -wave and  $\cos k_z$  for the  $s^{\pm}$  case. In Fig. 3 (c)-(f), results for these pair-field susceptibilities versus temperature are shown for different values of  $t_{\perp}$ . For  $t_{\perp} = 0.5$ , the  $d$ -wave response is larger than the  $s^{\pm}$  susceptibility. For  $t_{\perp} = 1$ , both channels are almost degenerate, while for  $t_{\perp} = 2$ , the  $s^{\pm}$  is the leading response and diverges at a relatively high temperature around  $0.05t$ . For  $t_{\perp} = 3$ , the pair-field response is significantly weakened. This near-degeneracy of the  $d_{x^2-y^2}$  and  $s^{\pm}$  pair-field correlations for intermediate values of  $t_{\perp}/t$  has been similarly observed in fluctuation-exchange calculations of realistic 5-orbital model calculations of the iron-pnictides [5,10].

A further analysis of the pairing interaction in the bilayer model [16] shows that the observed  $t_{\perp}$ -dependence

of the pairfield susceptibilities can be understood in terms of the  $t_{\perp}$ -dependence of the spin-fluctuation spectral weight. For small  $t_{\perp}$ , the intra-layer spin fluctuations are dominant and give rise to the  $d_{x^2-y^2}$  response. As  $t_{\perp}$  increases the dominant spin-fluctuations change from intra- to inter-layer, which give rise to the  $s^{\pm}$  pairing. For large  $t_{\perp} \gtrsim 3$ , the inter-layer spin fluctuations become gapped and contribute less to the pairing.

To conclude, we have reviewed dynamic cluster quantum Monte Carlo simulations of models of unconventional superconductors, including a 2D Hubbard model with charge stripes and a bilayer Hubbard model with multiple Fermi surfaces. We have shown that charge stripes in the 2D Hubbard model can lead to a significant enhancement of superconductivity. For the bilayer model, we have found a transition of the leading pairing instability from a  $d_{x^2-y^2}$ -wave to an  $s^{\pm}$  state with increasing inter-layer hopping  $t_{\perp}/t$ . We have also discussed how the superconducting behavior of these models can be understood in terms of a spin-fluctuation picture.

**Acknowledgements** We would like to acknowledge useful discussions with D.J. Scalapino, T.C. Schulthess, G. Alvarez and M. Summers. This research was conducted at the Center for Nanophase Materials Sciences, which is sponsored at Oak Ridge National Laboratory by the Office of Basic Energy Sciences, U.S. Department of Energy. This research was enabled by computational resources of the Center for Computational Sciences at Oak Ridge National Laboratory.

## References

- Anderson, P.: Science **235**, 1196 (1987)
- Bouadim, K., Batrouni, G.G., Hébert, F., Scalettar, R.T.: Phys. Rev. B **77**, 144,527 (2008)
- Bulut, N., Scalapino, D., Scalettar, R.: Phys. Rev. B **45**, 5577 (1992)
- Dos Santos, R.: Phys. Rev. B **51**, 15,540 (1995)
- Graser, S., Maier, T., Hirschfeld, P., Scalapino, D.: New J. Phys. **11**, 025,016 (2009)
- Hettler, M., Tahvildar-Zadeh, A., Jarrell, M., Pruschke, T., Krishnamurthy, H.: Phys. Rev. B **58**, R7475 (1998)
- Hetzl, R.E., von der Linden, W., Hanke, W.: Phys. Rev. B **50**, 4159 (1994)
- Jarrell, M., Maier, T., Huscroft, C., Moukouri, S.: Phys. Rev. B p. 195130 (2001)
- Kugel, K.I., Rakhmanov, A.L., Sboychakov, A.O., Poccia, N., Bianconi, A.: Phys. Rev. B **78**, 165,124 (2008)
- Kuroki, K., Onari, S., Arita, R., Usui, H., Tanaka, Y., Kontani, H., Aoki, H.: Phys. Rev. Lett. **101**, 087,004 (2008)
- Liechtenstein, A.I., Mazin, I.I., Andersen, O.K.: Phys. Rev. Lett. **74**, 2303 (1995)
- Maier, T., Alvarez, G., Summers, M., Schulthess, T.: Phys. Rev. Lett. **104**, 247,001 (2010)
- Maier, T., Jarrell, M., Pruschke, T., Hettler, M.: Rev. Mod. Phys. **77**, 1027 (2005)
- Maier, T., Jarrell, M., Scalapino, D.: Phys. Rev. Lett. **96**, 047,005 (2006)

- 
15. Maier, T., Jarrell, M., Scalapino, D.: Phys. Rev. B **74**, 094,513 (2006)
  16. Maier, T., Scalapino, D.: preprint arXiv:1107.0401 (2011)
  17. Scalettar, R., Cannon, J., Scalapino, D., Sugar, R.: Phys. Rev. B **50**(18), 13,419 (1994)
  18. Zhang, F., Rice, T.: Phys. Rev. B **37**, R3759 (1988)